Volume change determination of metastatic lung tumors in CT images using 3-D template matching

Robert D. Ambrosini[1], Peng Wang[2], and Walter G. O'Dell[1,3]

Departments of [1]Biomedical Engineering and [3]Radiation Oncology, University of Rochester, Rochester, NY 14642-8647, USA
[2]Department of Radiation Oncology, University of Michigan, Ann Arbor, MI 48109, USA

ABSTRACT

The ability of a clinician to properly detect changes in the size of lung nodules over time is a vital element to both the diagnosis of malignant growths and the monitoring of the response of cancerous lesions to therapy. We have developed a novel metastasis sizing algorithm based on 3-D template matching with spherical tumor appearance models that were created to match the expected geometry of the tumors of interest while accounting for potential spatial offsets of nodules in the slice thickness direction. The spherical template that best-fits the overall volume of each lung metastasis was determined through the optimization of the 3-D normalized cross-correlation coefficients (NCCC) calculated between the templates and the nodules. A total of 17 different lung metastases were extracted manually from real patient CT datasets and reconstructed in 3-D using spherical harmonics equations to generate simulated nodules for testing our algorithm. Each metastasis 3-D shape was then subjected to 10%, 25%, 50%, 75% and 90% scaling of its volume to allow for 5 possible volume change combinations relative to the original size per each reconstructed nodule and inserted back into CT datasets with appropriate blurring and noise addition. When plotted against the true volume change, the nodule volume changes calculated by our algorithm for these 85 data points exhibited a high degree of accuracy (slope = 0.9817, R^2 = 0.9957). Our results demonstrate that the 3-D template matching method can be an effective, fast, and accurate tool for automated sizing of metastatic tumors.

Keywords: Lung, CAD development

1. INTRODUCTION

Lung metastatic disease is a common result of many primary cancer types that can frequently lead to loss of life as well as cause a multitude of considerable complications for patients if not addressed promptly and effectively. Regular screenings are crucial in identifying metastatic disease early enough to optimize treatment efficacy and patient outcome where computed tomography (CT) is the current imaging modality of choice as it has been shown to be the most sensitive in detecting pulmonary nodules[1-10]. However, the presence of small lung nodules on CT scans does not necessarily alone provide confidence that a patient possesses lung metastases since most small lung nodules are caused by benign processes[11-13]. The indeterminate nature of radiographic pulmonary nodules as a clinical finding was illustrated in the Early Lung Cancer Action Project (ELCAP) study where among the 233 of the 1000 initial subjects that presented with 1 to 6 pulmonary nodules on their first screening only 27 (12%) of these subjects actually had malignant lung disease[3]. A major aspect of the difficulty in diagnosing patients based on the radiographic appearance of small nodules is that, with the exception of calcification, nodule morphologic characteristics do not provide clear indication for distinguishing benign from malignant processes[14].

Pulmonary nodule growth rate, on the other hand, has been discovered to be an early and reliable predictor of nodule malignancy[10,15-17]. In particular, malignant growths are distinguishable from benign nodules using the doubling time (DT) values that can be derived from growth rate information[18]. Malignant tumors in the lung were found normally to have DTs between 30 days and 14 months while benign nodules typically take longer than 14 months to double in volume[17,19-21]. Along these same lines, a malignancy risk of less than 10% has been estimated for nodules lacking a measurable increase in nodule volume over a 6-month period[22]. Furthermore, the recording of growth in nodules less

than 10 mm in diameter has been recommended as a condition before attempting biopsy to confirm the diagnosis of a malignant lesion[3]. Growth rate data can also enable the prioritizing of lung metastases on the basis of relative aggressiveness where the more aggressive nodules can be administered local treatment first in patients with too many metastases to have them all treated with stereotactic radiosurgery in a single therapy session. Similarly, ascertaining the change in nodule size post-treatment is essential to clinicians for establishing tumor response to therapy. As a result, the accurate sizing of lung nodules across serial CT scans and subsequent growth rate determination can play a significant role in the clinical evaluation process for cancerous lung lesions.

Deleted: the

Deleted: ment of

In general, the clinical approach to nodule sizing has been unidimensional or bidimensional where the diameter or cross-sectional area of the nodule is measured by the radiologist using manual drawing software. Diameter and cross-sectional area measurements can then be utilized to approximate nodule volume and doubling time through the implementation of either a spherical, elliptical, or irregularly-shaped (perimeter-based) model for the nodule[23]. There are inherent concerns with how these common manual methods for tumor sizing are time-consuming and introduce user subjectivity and other measurement errors inherent with the 2-D image viewing of a 3-D object. Numerous studies have demonstrated that human-reader driven measurements of pulmonary nodules suffer from substantial intra- and interobserver variability[24-27]. When used on CT scans of the lung, three-dimensional volume measuring techniques appear to reduce user subjectivity and overall measurement error as compared to conventional unidimensional or bidimensional techniques[13,15,27-29]. Moreover, recent evidence indicates that the availability of automated or semi-automated volume calculation tools to radiologists can decrease noticeably the variability of pulmonary nodule volume measurements[11-12,30]. Consequently, the evidence suggests that there is a distinct niche that could be filled by a computer-aided diagnosis (CAD) system with the ability to perform accurate 3-D volume assessments of pulmonary nodules.

Deleted: (DT)

Existing CAD approaches to the sizing of pulmonary nodules have centered primarily around either segmentation-based or model-based methods[10,15,31-33]. Segmentation-based methods typically involve intensity thresholding followed by voxel counting and they benefit from their capacity to handle irregular 3-D nodules shapes. However, segmentation-based methods can be affected by different CT scanner parameters due to their dependence upon the absolute CT values and it has been shown that they experience inaccuracies related to the fraction of partial volume voxels[31]. Model-based methods allow for 3-D volume determination without the explicit segmentation of nodules and can be more generalizable because they avoid dependence upon the absolute CT values, but they are only effective if they represent successfully the radiographic morphology of the object to be detected in the majority of instances. Anisotropic sampling of CT data is also an issue for model-based methods where they must account for unequal resolution in all three dimensions in order to achieve accurate volume matching with a nodule's 3-D shape. Regardless of the approach, robustness with regard to a wide range of nodule volumes and the capacity to separate the nodule's 3-D borders from surrounding anatomical structures are integral factors in producing a successful volume measurement.

We have developed a fully-automated CAD approach for the sizing of lung metastases that is based on the observation that pulmonary nodules appear in CT images as structures with approximately spherical 3-D intensity profiles[34]. Our fully-automated algorithm calculates the volume of pulmonary nodules by matching their morphology in 3-D with spherical tumor appearance models. The purpose of this paper is to validate the ability of our algorithm to improve the accuracy of volume measurements for lung metastases and in turn, allow for the direct calculation of nodule growth rates using repeated CT scans for the same patient. This more detailed knowledge of the absolute size and relative aggressiveness of multiple lung metastases within each patient offered by our algorithm will help clinicians provide earlier diagnoses and better tailor treatment strategies to promote enhanced quality of life and prolonged survival.

2. METHODS

Our algorithm calculates the volume of a lung metastasis by matching its size on a sub-voxel level to 3-D spherical templates designed to represent accurately the typical appearance of a metastasis within a CT dataset[34]. Spherical templates were generated to incorporate partial volume effects in both the in-plane and slice thickness directions. Four different spatial models were utilized for each size template to represent possible nodule partial volume effect

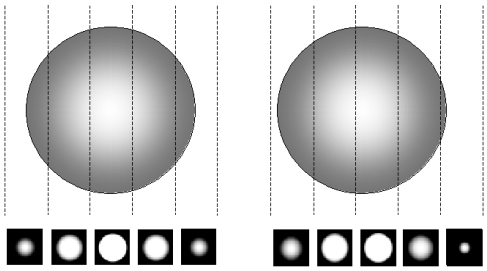

Figure 1. Models illustrating the variations in appearance of a sphere on simulated CT image slices caused by changes in position of the central image slice. Left pair: central image slice intersecting exact center of sphere. Right pair: central image slice shifted one-third of the slice thickness from the exact center of sphere.

orientations in the slice thickness direction where one spatial model placed the central CT slice exactly through the center of the spherical template while the other three models offset the center of the sphere from the central slice by one-half the slice thickness and in equal and opposite directions by one-third the slice thickness (see Figure 1). Furthermore, the spherical templates included zero padding in both the in-plane and slice thickness direction that was equal in width to twice the in-plane voxel size in order to ensure that metastases did not match with erroneously small spherical templates.

A normalized cross-correlation coefficient (NCCC) was calculated to identify the degree of similarity between the lung metastasis and the different sized spherical templates:

$$\bar{x} = \frac{1}{n}\sum_{n=1}^{i} x_i \,,\; \bar{y} = \frac{1}{n}\sum_{n=1}^{i} y_i$$

$$S_{xx}^2 = \frac{1}{n-1}\sum_{i=1}^{n}\left(x_i - \bar{x}\right)^2 \,,\; S_{yy}^2 = \frac{1}{n-1}\sum_{i=1}^{n}\left(y_i - \bar{y}\right)^2 \qquad (1)$$

$$Cov_{xy} = \frac{1}{n-1}\sum_{i=1}^{n}\left(x_i - \bar{x}\right)\left(y_i - \bar{y}\right)$$

$$NCCC = \frac{Cov_{xy}}{\sqrt{S_{xx}^2 \cdot S_{yy}^2}}$$

where dataset "x" consists of the voxel intensity values for the 3-D spherical template and dataset "y" consists of the voxel intensity values for the 3-D image region containing the lung metastasis that is actively being sized. The spherical template that produced the optimal NCCC value (closest to one) was considered to provide the most accurate estimate of nodule volume. The initial approximation of the center of the nodule to be sized can either be selected manually or generated by an automated lung nodule detection algorithm's output[34]. For the purpose of guaranteeing that the spherical template matching process was properly aligned in 3-D for the most accurate sizing of each nodule, NCCC values were calculated throughout a 125-voxel neighborhood around the selected nodule center with the capability of also searching further neighboring voxels depending on the trend of NCCC values within the initial volume of interest (VOI). The computational cost for searching these additional voxels was minimal with the entire sizing process taking several seconds per nodule running in MATLAB 7.2[35] on a Power Mac G5 with quad 2.5 GHz processors and 4 gigabytes of RAM.

In order to validate the accuracy of our metastasis sizing approach, simulated lung CT nodules were generated based on the 3-D appearance of confirmed lung metastases found within patient CT datasets acquired at our institution. A total of 17 lung metastases were contoured manually from four different patient CT datasets. The spherical coordinates for the points that compose the borders of these extracted metastases were identified on each CT slice. The

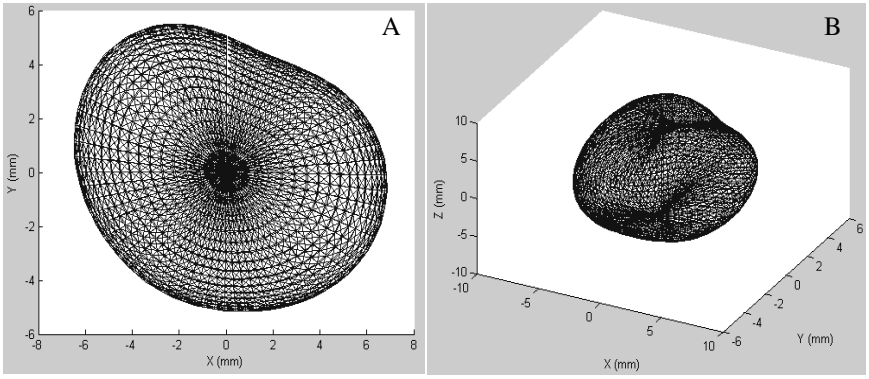

Figure 2. Example reconstruction of one of the 17 extracted CT lung metastases that were used as simulated nodules with views from the slice thickness [A] and oblique [B] directions. 3-D surface contour points were generated through the utilization of spherical harmonics equations.

use of spherical harmonics then allowed the reconstruction of the full 3-D structure of each metastasis from these 2-D samplings of its shape. The spherical harmonics values that defined uniquely each 3-D metastasis system were calculated using the following equations:

$$r = \sum_{l=0}^{3} \sum_{m=-l}^{l} A_{l,m}\, Y_l^m(\theta, \varphi) \tag{2}$$

$$Y_l^m(\theta,\phi) = \sqrt{\frac{2l+1}{4\pi}\frac{(l-m)!}{(l+m)!}} P_l^m(\cos\theta) e^{im\phi}$$

where r is the nodule radius, A represents the constants determined from the extracted nodule contouring, Y is the spherical harmonic, θ is the polar (colatitudinal) coordinate, ϕ is the azimuthal (longitudinal) coordinate, and P is an associated Legendre polynomial. After the 3-D reconstruction of each metastasis, the volume was determined by dividing the nodule into a combination of pyramids defined by the data points used to generate its irregular 3-D shape. The volume of each individual pyramid was calculated using vector mathematics and the summation of these values was designated as the gold standard volume for that tumor. In addition to the original reconstructed volume, each metastasis 3-D shape was subjected to 10%, 25%, 50%, 75% and 90% scaling of its volume to allow for 5 possible volume change combinations relative to the original size per each reconstructed nodule. After reconstruction, the nodules were adjusted randomly for positional shifts in the slice thickness direction, converted into 2-D slice representations, and inserted strategically into a healthy region within a different patient's CT dataset. Finally, the inserted nodules were blurred with a Gaussian filter to duplicate the point spread function of a standard clinical imaging scanner and Gaussian noise was added using a standard deviation equal to the average intrinsic noise of the utilized patient CT datasets.

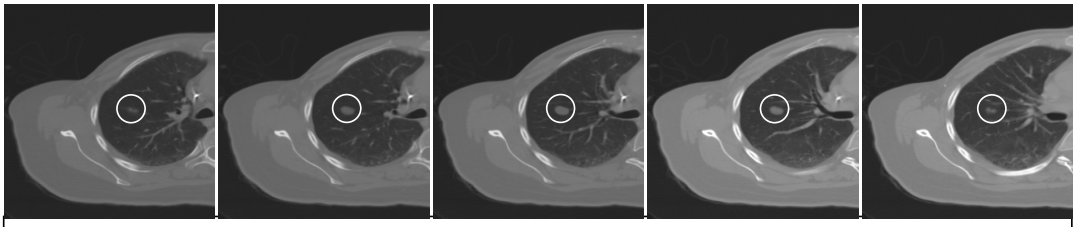

Figure 3. Five sequential CT slices illustrating the insertion of the example simulated nodule (circled) that was shown in Figure 1 into a healthy region of a different patient's CT dataset where Gaussian blurring and Gaussian noise are then added.

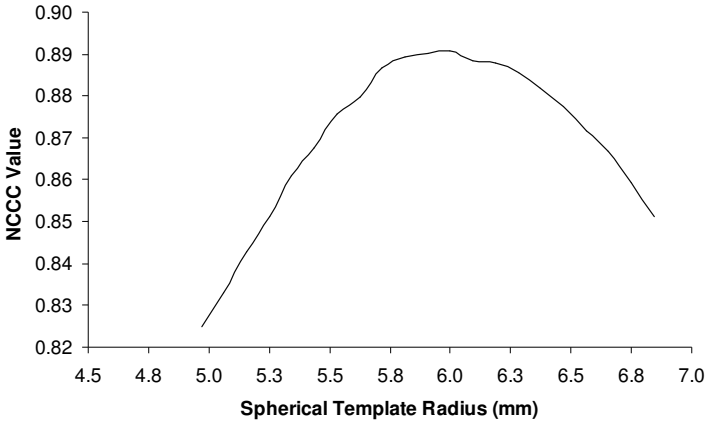

Figure 4. Normalized cross-correlation coefficient (NCCC) curve for example simulated nodule shown in Figures 1 and 2 where reconstructed metastasis is found to best match a spherical template with a radius of approximately 6.0 mm and corresponding volume of 904.8 mm^3 as compared to a gold standard volume of 867.8 mm^3 (4.1% deviation).

The lung CT images used in this work were collected with a standard GE Genesis Lightspeed CT clinical scanner with slice thickness and separation 3 mm, in-plane resolution 0.9375 mm, tube voltage 120 kV, and tube current 70 – 120 mA. Images were obtained during 20 to 30 second end-expiration breath-hold, with no injected contrast.

3. RESULTS

The principal rationale behind utilizing simulated nodules that had been reconstructed in 3-D from the contours of lung metastases found within actual patient CT datasets was to produce 3-D intensity profiles representative of real lung metastases for testing our sizing algorithm. Figure 2 demonstrates the ability of the 3-D reconstruction based on spherical harmonics equations to provide a 3-D nodule shape that is consistent with the irregularities of lung metastasis geometry found within patient CT datasets. Figure 3 displays the sequential 2-D slice appearance of the reconstructed nodule shown in Figure 2 after it has been inserted into the healthy region of a different patient's CT dataset and subjected to Gaussian blurring and the addition of Gaussian noise. The relationship between the NCCC value and the spherical templates of varying radii is then shown for this simulated nodule in Figure 4 where the best-fit template possesses a volume equal to 904.8 mm^3 as compared to the gold standard volume of 867.8 mm^3 (4.1% deviation).

The ability to differentiate often subtle changes in overall 3-D nodule volume is the critical factor that underlies the possible use of our algorithm as a clinical tool to aid radiologists in identifying metastatic processes and monitoring the therapeutic response of treated lesions. Figure 5 shows the volume change values calculated through best-fit template matching compared to the true volume changes determined during the 3-D nodule reconstruction process. The data displayed in Figure 5 illustrate the general overall accuracy of our best-fit spherical template matching-based approach in producing volume change values when judged against the gold standard volume change values (slope = 0.9817, $R^2 = 0.9957$).

4. CONCLUSIONS

We have developed a novel approach to 3-D lung nodule sizing in CT scans that has the capacity to determine accurately small changes in volume at a low computational cost. Simulated nodules reconstructed from the actual 3-D morphology and intensity profiles of real patient lung metastases were employed to evaluate the efficacy of our algorithm. The validation of our algorithm's volume change calculation accuracy in this manner reduces a great deal of the ambiguity and subjectivity that is encountered when radiologist measurements are utilized as the gold standard for nodule size. Similarly, testing with simulated nodules inserted into patient CT lung datasets eliminates dependence upon validation through phantom studies where success with synthetic nodules does not ensure *in vivo* accuracy due to patient motion effects, less distinct nodule borders, and intricate surrounding anatomy affecting results[36].

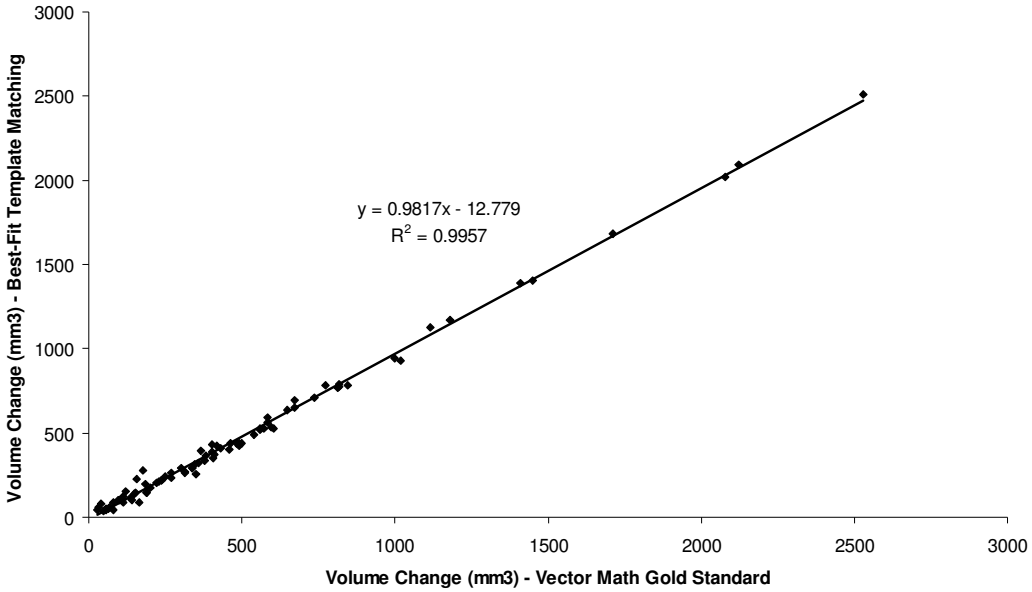

Figure 5. Volume change data collected using simulated metastatic lung nodules that were reconstructed from contouring of 17 different real patient lung metastases. Each reconstructed 3-D nodule shape was scaled at 10%, 25%, 50%, 75%, and 90% of its original volume and compared to the original simulated nodule volume to provide 5 separate volume change calculations per simulated nodule shape, resulting in 85 total volume change data points. The volume changes generated through the best-fit template matching method are compared at each of these 85 data points to the simulated nodule volume changes derived from vector mathematics calculations, which is regarded as the gold standard in this work. Straight line shown is best-fit trendline generated for displayed data points. Individual metastasis volumes ranged from 35.4 to 2786.3 mm^3 (mean = 537.5 mm^3) while volume change magnitudes ranged from 35.4 to 2507.7 mm^3 (mean = 460.7 mm^3).

In this study, volume change was selected as the metric by which to analyze our algorithm as consistency in computing the change in size of a lung nodule has greater clinical relevance than accuracy in absolute volume determination[30]. The volume change measurement results presented here demonstrate that our 3-D spherical template matching-based algorithm can be implemented as a precise and reliable means of calculating automatically the volume change of metastatic lung nodules within CT datasets. These positive results are especially encouraging given the large anisotropic voxel size of the CT data that was tested. Future work will focus upon combining our low computational cost sizing method with automated image registration and nodule labeling approaches for the purpose of providing a clinical tool to assist radiologists in more definitively diagnosing and monitoring metastatic tumors.

ACKNOWLEGDMENTS

Robert Ambrosini is a trainee in the Medical Scientist Training Program, NIH T32 GM-07356.

REFERENCES

[1] Kaneko, M., Eguchi, K., Ohmatsu, H., Kakinuma, R., Naruke, T., Suemasu, K., and Moriyama, N., "Peripheral lung cancer: screening and detection with low-dose spiral CT versus radiography," Radiology 201, 798-802 (1996).
[2] Sone, S., Takashima, S., Li, F., Yang, Z., Honda, T., Maruyama, Y., Hasegawa, M., Yamanda, T., Kubo, K., Hanamura, K., and Asakura, K., "Mass screening for lung cancer with mobile spiral computed tomography scanner," Lancet 351, 1242-1245 (1998).

[3] Henschke, C.I., McCauley, D.I., Yankelevitz, D.F., Naidich, D.P., McGuinness, G., Miettinen, O.S., Libby, D., Pasmantier, M., Koizumi, J., Altorki, N., and Smith, J.P., "Early Lung Cancer Action Project: overall design and findings from baseline screening," Lancet 354, 99-105 (1999).
[4] Sone, S., Li, F., Takashima, S., Maruyama, Y., Hasegawa, M., Wang, J.C., Kawakami, S., and Honda, T., "Characteristics of small lung cancers invisible on conventional chest radiography and detected by population based screening using spiral CT," Br. J. Radiol. 73, 137-145 (2000).
[5] Nawa, T., Nakagawa, T., Kusano, S., Kawasaki, Y., Sugawara, Y., and Nakata, H., "Lung cancer screening using low-dose spiral CT: results of baseline and 1-year follow-up studies," Chest 122, 15-20 (2002).
[6] Diederich, S., Wormanns, D., Semik, M., Thomas, M., Lenzen, H., Roos, N., and Heindel, W., "Screening for early lung cancer with low-dose spiral CT: prevalence in 817 asymptomatic smokers," Radiology 222, 773-781 (2002).
[7] Swensen, S.J., Jett, J.R., Sloan, J.A., Midthun, D.E., Hartman, T.E., Sykes, A., Aughenbaugh, G.L., Zink, F.E., Hillman, S.L., Noetzel, G.R., Marks, R.S., Clayton, A.C., and Pairolero, P.C., "Screening for lung cancer with low-dose spiral computed tomography," Am. J. Respir. Crit. Care Med. 165, 508-513 (2002).
[8] Sobue, T., Moriyama, N., Kaneko, M., Kusumoto, M., Kobayashi, T., Tsuchiya, R., Kakinuma, R., Ohmatsu, H., Nagai, K., Nishiyama, H., Matsui, E., and Eguchi, K., "Screening for lung cancer with low-dose helical computed tomography: anti-lung cancer association project," J. Clin. Oncol. 20, 911-920 (2002).
[9] Awai, K., Murao, K., Ozawa, A., Komi, M., Hayakawa, H., Hori, S., and Nishimura, Y., "Pulmonary nodules at chest CT: effect of computer-aided diagnosis on radiologists' detection performance," Radiology 230, 347-352 (2004).
[10] Okada, K., Comaniciu, D., and Krishnan, A., "Robust anisotropic gaussian fitting for volumetric characterization of pulmonary nodules in multislice CT," IEEE Trans. Med. Imag. 24(3), 409-423 (2005).
[11] Marten, K. and Engelke, C., "Computer-aided detection and automated CT volumetry of pulmonary nodules," Eur. Radiol. 17, 888-901 (2007).
[12] Therasse, P., Arbuck, S.G., Eisenhauer, E.A., Wanders, J., Kaplan, R.S., Rubinstein, L., Verweij, J., Van Glabbeke, M., van Oosterom, A.T., Christian, M.C., and Gwyther, S.G., "New guidelines to evaluate the response to treatment in solid tumors," J. Natl. Cancer Inst. 92, 205-216 (2000).
[13] Yankelevitz, D.F., Reeves, A.P., Kostis, W.J., Zhao, B., and Henschke, C.I., "Small pulmonary nodules: volumetrically determined growth rates based on CT evaluation," Radiology 217, 251-256 (2000).
[14] Erasmus, J.J., Connolly, J.E., McAdams, H.P., and Roggli, V.L., "Solitary pulmonary nodules. Part I. Morphologic evaluation for differentiation of benign and malignant lesions," RadioGraphics 20, 43-58 (2000).
[15] Kostis, W.J., Reeves, A.P., Yankelevitz, D.F., and Henschke, C.I., "Three-dimensional segmentation and growth-rate estimation of small pulmonary nodules in helical CT images," IEEE Trans. Med. Imag. 22(10), 1259-1274 (2003).
[16] Collins, V.P., Loeffler, R.K., and Tivey, H., "Observations on growth rates of human tumors," AJR 76, 988-1000 (1956).
[17] Nathan, M.H., Collins, V.P., and Adams, R.A., "Differentiation of benign and malignant pulmonary nodules by growth rate," Radiology 79, 221-231 (1962).
[18] Schwartz, M., "A biomathematical approach to clinical tumor growth," Cancer 14(6), 1272-1294 (1961).
[19] Weiss, W., "Peripheral measurable bronchogenic carcinoma: growth rate and period of risk after therapy," Am. Rev. Respir. Dis. 103, 198-208 (1971).
[20] Aoki, T., Nakata, H., Watanabe, H., Nakamura, K., Kasai, T., Hashimoto, H., Yasumoto, K., and Kido, M., "Evolution of peripheral lung adenocarcinomas: CT findings correlated with histology and tumor doubling time," AJR 174, 763-768 (2000).
[21] Ko, J.P., Rusinek, H., Jacobs, E.L., Babb, J.S., Betke, M., McGuinness, G., and Naidich, D.P., "Small pulmonary nodules: volume measurement at chest CT – phantom study," Radiology 228, 864-870 (2003).
[22] Libby, D.M., Smith, J.P., Altorki, N.K., Pasmantier, M.W., Yankelevitz, D., and Henschke, C.I., "Managing the small pulmonary nodule discovered by CT," Chest 125, 1522-1529 (2004).
[23] Winer-Muram, H.T., Jennings, S.G., Tarver, R.D., Aisen, A.M., Tann, M., Conces, D.J., and Meyer, C.A., "Volumetric growth rate of stage I lung cancer prior to treatment: serial CT scanning," Radiology 223, 798-805 (2002).
[24] Marten, K., Auer, F., Schmidt, S., Kohl, G., Rummeny, E.J., and Engelke, C., "Inadequacy of manual measurements compared to automated CT volumetry in assessment of treatment response of pulmonary metastases using RECIST criteria," Eur. Radiol. 16, 781-790 (2006).
[25] Bogot, N.R., Kazerooni, E.A., Kelly, A.M., Quint, L.E., Desjardins, B., and Nan, B., "Interobserver and intraobserver variability in the assessment of pulmonary nodule size on CT using film and computer display methods," Acad. Radiol. 12, 948-956 (2005).

[26] Meyer, C.R., Johnson, T.D., McLennan, G., *et al.* "Evaluation of lung MDCT nodule annotation across radiologists and methods," Acad. Radiol. 13, 1254-1265 (2006).
[27] Reeves, A.P., Biancardi, A.M., Apanasovich, T.V., Meyer, C.R., MacMahon, H., van Beek, E.J.R., Kazerooni, E.A., Yankelevitz, D., McNitt-Gray, M.F., McLennan, G., Armato III, S.G., Henschke, C.I., Aberle, D.R., Croft, B.Y., and Clarke, L.P., "The Lung Image Database Consortium (LIDC): A comparison of different size metrics for pulmonary measurements," Acad. Radiol. 14, 1475-1485 (2007).
[28] Yankelevitz, D.F., Gupta, R., Zhao, B., and Henschke, C.I., "Small pulmonary nodules: evaluation with repeat CT – preliminary experience," Radiology 212, 561-566 (1999).
[29] Zhao, B., Schwartz, L.H., Moskowitz, C.S., Ginsberg, M.S., Rizvi, N.A., and Kris, M.G., "Lung cancer: computerized quantification of tumor response – initial results," Radiology 241, 892-898 (2006).
[30] Goodman, L.R., Gulsun, M., Washington, L., Nagy, P.G., and Piacsek, K.L., "Inherent variability of CT lung nodule measurements in vivo using semiautomated volumetric measurements," AJR 186, 989-994 (2006).
[31] Reeves, A.P., Chan, A.B., Yankelevitz, D.F., Henschke, C.I., Kressler, B., and Kostis, W.J., "On measuring the change in size of pulmonary nodules," IEEE Trans. Med. Imag. 25(4), 435-450 (2006).
[32] Bomsztyk, E.D. and Rusinek, H., "Volumetric analysis of lung nodules using a hybrid algorithm," Proc. SPIE 5370, 22-29 (2004).
[33] Kawata, Y., Niki, N., Ohmatsu, H., Kusumoto, M., Kakinuma, R., Mori, K., Yamada, K., Hishiyama, H., Kaneko, M., and Moriyama, N., "A computerized approach for estimating pulmonary nodule growth rates in three-dimensional thoracic CT images based on CT density histogram," Proc. SPIE 5747, 872-882 (2005).
[34] Wang, P., DeNunzio, A., Okunieff, P., and O'Dell, W.G., "Lung metastases detection in CT images using 3D template matching," Med. Phys. 34(3), 915-922 (2007).
[35] MathWorks, MATLAB (The MathWorks Inc.).
[36] de Hoop, B., Gietema, H., van Ginneken, B., Zanen, P., Groenewegen, G., and Prokop, M., "A comparison of six software packages for evaluation of solid lung nodules using semi-automated volumetry: What is the minimum increase in size to detect growth in repeated CT examinations," Eur. Radiol., (2008).